Dev. Neurobiol. 71, 584-593, 2011

Systems Biology of Symmetry-Breaking during Neuronal Polarity Formation

Running title: Modelling Neuronal Symmetry-Breaking

Naoyuki Inagaki[1,*], Michinori Toriyama[1], Yuichi Sakumura[2]

[1]Graduate School of Biological Sciences and [2]Graduate School of Information Science, Nara Institute of Science and Technology, Ikoma 630-0192, Japan

[*]Correspondence to: Naoyuki Inagaki

Graduate School of Biological Sciences, Nara Institute of Science and Technology, Ikoma 630-0192, Nara, Japan

e-mail: ninagaki@bs.naist.jp Tel: 81-743-72-5466 Fax: 81-743-72-5509

This research was supported in part by JSPS KAKENHI, the Global COE Program at NAIST (MEXT), Osaka Medical Research Foundation for Incurable Diseases, and NAIST Interdisciplinary Frontier Research Project.

ABSTRACT

Polarization, in which a single axon and multiple dendrites are formed, is crucial for neuronal functions, and symmetry-breaking is the initial step of this process. Accumulating studies have revealed a number of molecules that act asymmetrically in neurons, and thereby regulate neuronal polarity. Thus, one of the major goals of current research is to understand how asymmetric signals are generated during the symmetry-breaking step. Current models of neuronal symmetry-breaking generally involve “local activation” for induction of axon outgrowth and “global inhibition” to suppress formation of multiple axons, and can be categorized into “one-takes-all” and “activator-inhibitor” models. Both types of model incorporate a positive feedback loop to execute local activation, but differ in the manner of global inhibition. Quantitative experimentation combined with computational modeling is a powerful strategy in systems biology, and analyses in this direction have begun to yield a more profound understanding of how neurons break their symmetry during polarity formation.

Key words: neuronal polarity; feedback loop; quantitative modeling; shootin1; stochasticity

INTRODUCTION

Neurons develop polarity by forming a single axon and multiple dendrites (Craig and Banker, 1994; Winckler and Mellman, 1999; Da Silva and Dotti, 2002; Horton and Ehlers, 2003). The processes of neuronal polarization have been extensively studied using cultured hippocampal neurons as a model system (Dotti et al., 1988; Craig and Banker, 1994). These neurons first form several immature neurites that are similar in length, and at this stage the neurons appear symmetric (stage 2). One of these neurites then outgrows its siblings to break the neuronal symmetry, and acquires axonal characteristics (stage 3); this break in symmetry is the initial step of neuronal polarization. The other immature neurites later become dendrites (stage 4) and neurons finally establish polarity (stage 5). Cultured hippocampal neurons execute these polarization processes in the absence of apparent external directional cues. Notably, they re-polarize even when polarity is disrupted by axonal transection at stages 3 or 4 (Goslin and Banker, 1989; Bradke and Dotti, 2000). Hippocampal neurons therefore appear to use a robust intrinsic mechanism to break symmetry, which may guarantee polarization not only *in vitro* but also *in vivo*. Interestingly, cultured non-neuronal cells, including neutrophils (Zigmond et al., 1981; Weiner et al., 2002), keratocytes (Yam et al., 2007) and fibroblasts (Symons and Mitchison, 1991), also have the capacity to break symmetry in the absence of an external asymmetric cue. In these cell types, and probably also in neuronal cells, asymmetric cues are thought only to induce a preferred directionality upon pre-existing cellular polarity, which is generated by default (Sohrmann and Peter, 2003; Wedlich-Soldner and Li, 2003; Yam et al., 2007).

As described in recent excellent reviews (Arimura and Kaibuchi, 2007; Barnes and Polleux, 2009; Conde and Caceres, 2009; Tahirovic and Bradke, 2009), intensive

studies during the last decade have revealed a number of molecules that act asymmetrically in neurons, and thereby regulate neuronal polarity. Thus, one of the major goals of current research is to understand how asymmetric signals are generated during the symmetry-breaking step. The regulator molecules were identified, in many cases, by analyzing (1) selective accumulation/exclusion of the molecules/signals in the nascent axon and (2) effects of their over-expression/over-activation or repression/knockout/inhibition on the formation of axons and dendrites (Inagaki et al., 2001; Kunda et al., 2001; Shi et al., 2003; Jiang et al., 2005; Kishi et al., 2005; Yoshimura et al., 2005). Such a strategy has been useful to define key molecules involved in neuronal polarization. However, it is difficult to understand how they are asymmetrically distributed, without identifying explicitly the mechanistic components (molecules and their spatiotemporal behaviors) sufficient to comprise a system for the induction of neuronal symmetry-breaking. In this regard, integration of quantitative experimental data by computational modeling is an up-and-coming strategy for answering such problems in biological pattern formation (Mogilner et al., 2006; Iglesias and Devreotes, 2008; Lewis, 2008; Meinhardt, 2008).

For mathematical modeling, one advantage of neurons over other types of polarizing cells is that their morphology can be described in simple terms using a small number of parameters for neurite length (see below, Fig. 6D and E) (Samuels et al., 1996). In addition, recent technological advances in microscopy enable us to obtain quantitative spatiotemporal data about how molecules behave during neuronal polarization (Menager et al., 2004; Jacobson et al., 2006; Toriyama et al., 2006; Fivaz et al., 2008; Shimada et al., 2008; Shelly et al., 2010; Toriyama et al., 2010). Such live cell imaging data provide useful material for computational analysis. This review

outlines recent systems biological approaches which are beginning to uncover how neurons break their symmetry.

WHAT WE CAN LEARN FROM THE HODGKIN AND HUXLEY MODEL

Before describing the models of neuronal symmetry-breaking, we will explain briefly the model of Hodgkin and Huxley (1952), as it provides important guidance for systems biological approaches (Lewis and Ozbudak, 2007). There were many competing theories for action potential when Hodgkin and Huxley began their study. Through modeling analyses, they demonstrated that action potential is explained by potassium and sodium conductance. To show this, they quantified the dynamics of potassium conductance (Fig. 1A) and sodium conductance (Fig. 1B), and fitted the two components to mathematical models. The parameters of the model components were derived entirely from quantitative experimental data without any adjustment, and the model components described the experimental data with high accuracy (Fig. 1A and B, lines and circles). They then combined both model components without any adjustment, thereby showing good agreement between the reconstructed action potential and the experimentally observed action potential (Fig. 1C). In addition, the validity of the action potential model was supported by the large number (eight) of agreements between the model predictions and experimental observations (Hodgkin and Huxley, 1952). Much later, the molecular nature of the mechanistic components was understood. Thus, it is thought that the importance of components in a system can only be judged by such a quantitative analysis, with no assumptions and no arbitrary adjustment of model parameters (Hodgkin and Huxley, 1952; Lewis and Ozbudak, 2007; Meinhardt, 2008). The Hodgkin and Huxley model also tells us that a large

number of agreements between the model predictions and experimental observations is an important point for persuasive mathematical models.

MODELS FOR NEURONAL SYMMETRY-BREAKING

Theoretical models have been developed to explain how an initially symmetric biological structure can be transformed into an asymmetric one. Turing (1952) presented a model in which the interaction between two substances having different diffusion rates can give rise to spatial concentration patterns from almost uniform initial distributions. Refined extensions of this model were proposed based on "local activation and global inhibition" (Meinhardt and Gierer, 2000; Kondo, 2002; Iglesias and Devreotes, 2008). Current models of neuronal symmetry-breaking generally incorporate this concept, with "local activation" for induction of axon outgrowth and "global inhibition" to suppress formation of multiple axons, and can be categorized into two types. We will refer to one type as the "one-takes-all" model, in which each neurite competes for a limited amount of a molecule(s) that activates neurite outgrowth (Fig. 2A). In this model, one of the neurites eventually wins in this competition by means of a positive feedback loop (circular and thick arrows), thereby leading to the depletion of the activator molecule in the cell body and the other neurites (thin arrows). The other type involves both an "activator" and an "inhibitor" of neurite outgrowth (Fig. 2B): a signal to induce neurite outgrowth becomes continuously activated within one neurite by a positive feedback loop (circular arrow), and this in turn generates a global inhibitory signal that propagates to the other neurites (white arrows). A key difference between the "one-takes-all" and "activator-inhibitor" models is that intra-neuritic anterograde transport is a critical component of the former model but is not important in

the latter. On the other hand, global propagation of an inhibitory signal is a key component in the latter model but is not involved in the former.

MOLECULES PROPOSED FOR THE "ACTIVATOR-INHIBITOR" MODEL

Numbers of molecules are proposed to act as signals in the "activator-inhibitor" model (Andersen and Bi, 2000; Bradke and Dotti, 2000; Arimura and Kaibuchi, 2007). The activators include phosphoinositide-3-kinase (PI3K) (Shi et al., 2003), phosphatidylinositol (3,4,5) triphosphate (PIP_3) (Menager et al., 2004), mPar3/mPar6/aPKC complex (Shi et al., 2003; Nishimura et al., 2005), Cdc42 (Schwamborn and Puschel, 2004; Nishimura et al., 2005), Rap1B (Schwamborn and Puschel, 2004), STEF/Tiam1 (Kunda et al., 2001; Nishimura et al., 2005), and Rac (Nishimura et al., 2005). On the other hand, molecules such as glycogen synthase kinase-3β (GSK-3β) (Jiang et al., 2005; Yoshimura et al., 2005), PTEN (Shi et al., 2003; Jiang et al., 2005) and Singar1 (Mori et al., 2007) are candidate inhibitors. Recently, Shelly et al. (2010) reported that the elevation of cAMP and cGMP in immature neurites promotes and suppresses axon formation, respectively. Changes in the level of cAMP resulted in opposite changes in the level of cGMP, and vice versa. Furthermore, local elevation of cAMP in one neurite resulted in cAMP reduction in all other neurites of the same neuron. These results suggest that cAMP and cGMP play roles in ensuring the generation of a single axon and multiple dendrites. So far, no mathematical analysis of the "activator-inhibitor" model has been reported. We will describe mathematical "one-takes-all" models in the following sections.

ENHANCED TRANSPORT-BASED "ONE-TAKES-ALL" MODELS

One of the earliest mathematical models of "one-takes-all" model was that constructed by Samuels et al. (1996) (Fig. 3A). They hypothesized the existence of a "determinant chemical" which is necessary for neurite outgrowth and is transported from the cell body to the neurite tips (black arrows). They also assumed that an increase in the neurite outgrowth velocity (white arrows) enhances the rate of the chemical's anterograde transport (dashed arrow). Thus, the anterograde transport constitutes a positive feedback loop with neurite outgrowth that amplifies the accumulation of the rate-limiting substance at the neurite tips. As the amount of the determinant chemical is limited, this accumulation leads to its depletion in other regions. Within a certain parameter range, their computational model neuron amplified an initial small asymmetric signal, and formed a single fast-growing neurite while the other neurites grew very slowly.

Fivaz et al. (2008) reported a positive feedback interaction between HRas and PI3K in neurite tips, based on which they constructed a computational model of neuronal symmetry-breaking (Fig. 3B). They hypothesized that the positive feedback between HRas and PI3K (circular arrows) enhances the anterograde transport of HRas (dashed arrow). As HRas activity induces neurite outgrowth, the enhancement of the HRas transport and HRas-induced neurite outgrowth constitute an additional positive feedback loop for competitive accumulation of HRas. In addition, 5% noise was introduced to the initial conditions of their model for consistent formation of a single axon, and stochasticity was also added to the model by assuming random fusion events of HRas-loaded vesicles with the plasma membrane. Based on these assumptions, their mathematical model successfully broke symmetry by forming a single axon and multiple dendrites. Furthermore, HRas overexpression and RNAi in the model

disturbed polarization, as observed in cultured neurons. It will be intriguing to determine whether the assumed enhanced transport and the stochasticities exist in neurons, and thus whether the feedback between HRas and PI3K is indeed involved in the symmetry-breaking step.

DIFFUSION-BASED "ONE-TAKES-ALL" MODEL

Toriyama et al. (2010) recently constructed a computational "one-takes-all" model of neuronal symmetry-breaking from only experimentally observed quantitative data, following the strategy of Hodgkin and Huxley (1952b). Shootin1 is one of the key proteins involved in neuronal polarization (Toriyama et al., 2006; Shimada et al., 2008). It becomes up-regulated during the symmetry-breaking step and undergoes a stochastic accumulation in multiple growth cones. Eventually it accumulates predominantly in a single neurite, which subsequently grows to become the axon. Accumulated shootin1 in growth cones induces neurite outgrowth by acting as a clutch molecule to produce a traction force (Shimada et al., 2008), whereas repressing shootin1 expression inhibits neuronal polarization (Toriyama et al., 2006).

Interestingly, shootin1 is stochastically transported from the cell body to growth cones as discrete boluses, and diffuses back to the cell body (Toriyama et al., 2006). Irregular arrival of shootin1 at the neurite tips causes large stochastic fluctuations in shootin1 concentration in the growth cones (Toriyama et al., 2010). As molecules diffuse in proportion to the steepness of their concentration gradient, and as the gradient in a neurite shaft would be inversely proportional to the neurite's length (Fig. 4A, pink trapezoids), it was assumed that shootin1 diffuses back more slowly in longer neurites (thin blue arrow) than in shorter neurites (thick blue arrow). Thus,

longer neurites would accumulate more shootin1 (Fig. 4B) if it is transported equivalently to all neurites (red arrows). Measurement of retrograde movement of shootin1 confirmed that shootin1 indeed diffuses back more slowly in longer neurites than in shorter ones (Toriyama et al., 2010). In addition, axonal transection experiments demonstrated that shootin1 accumulation in growth cones is neurite length-dependent, regardless of whether the neurites are axonal stumps or immature neurites.

To establish whether the neurite length-dependency of shootin1 accumulation is indeed explained by its anterograde transport and retrograde diffusion, the stochastic transport of shootin1 and its retrograde diffusion were quantified (Fig. 5A, upper panel, and Fig. 5B, red squares). The data were then fitted into mathematical models of the anterograde transport and retrograde diffusion. The parameters of these two models were derived entirely from the quantitative experimental data without any adjustment, and the models described the experimental data with good accuracy (Fig. 5A, lower panel, and Fig. 5B, blue line). Shootin1 concentration at neurite tips, calculated by integrating the two models (Fig. 5C, blue circles), was neurite length-dependent and showed a good agreement with the experimental data (Fig. 5C, red circles). These results suggest that the neurite length-dependent accumulation of shootin1 is quantitatively explained by its anterograde transport and retrograde diffusion.

The length-dependent shootin1 accumulation constitutes a positive feedback interaction with shootin1-induced neurite outgrowth (Fig. 4C). This feedback loop was assumed to amplify stochastic shootin1 signals in growth cones, thereby generating an asymmetric shootin1 signal for the symmetry-breaking step. To analyze the functional role of the feedback loop, shootin1 up-regulation and shootin1-induced

neurite outgrowth were quantified (Fig. 6A and B, red circles), and fitted to mathematical models. Again, the parameters of both models were derived entirely from quantitative experimental data, and the models described the experimental data with good accuracy (Fig. 6A, blue line, and Fig. 6B, blue circles). These models were then integrated, together with the model of neurite length-dependent shootin1 accumulation (Fig. 6C), into a model neuron (Fig. 6D). The resultant model neuron spontaneously broke symmetry, in good agreement with the experimental data (Fig. 5E). Furthermore, the model neuron simulated neuronal morphological changes observed under normal and modified conditions, including the disturbance of neuronal polarization by shootin1 overexpression and RNAi (Toriyama et al., 2006) and neurite length-dependent axon regeneration and formation (Goslin and Banker, 1989; Lamoureux et al., 2002). The validity of the model was supported by fifteen agreements between the model predictions and experimental data (Toriyama et al., 2010). These data suggest that the three components in this model – diffusion-based neurite-length-dependent shootin1 accumulation, shootin1-induced neurite outgrowth and shootin1 up-regulation – constitute a minimum mechanism sufficient to induce neuronal symmetry-breaking.

The diffusion-based system broke symmetry without an additional inhibitory molecule or enhanced transport proposed in the other models. Nevertheless, it is compatible with the other models, and may thus provide a mechanism of neuronal symmetry-breaking, to which other mechanisms can be added to increase the model's accuracy.

CONCLUDING REMARKS

The combination of quantitative experimentation and mathematical modeling is a powerful strategy in systems biology, and studies in this direction have begun to analyze neuronal symmetry-breaking. At present, the whole picture of the mechanism of the symmetry-breaking step remains unclear. Currently, there are a number of different (competing or complementary) models for initiating neuronal polarization, which will be tested in future studies. Many other molecules are thought to be involved in neuronal polarization in addition to those described here (Arimura and Kaibuchi, 2007; Barnes and Polleux, 2009; Tahirovic and Bradke, 2009). It is also important to link the external cue-dependent signaling with the intrinsic symmetry-breaking mechanism in order to explain the orderly regulated neuronal polarity in the brain. Because the system involved in neuronal symmetry-breaking is complicated, it would be reasonable to begin with a simple model and to proceed gradually to more sophisticated ones. Progress in physics, as well as the pioneering work of Hodgkin and Huxley, tells us that careful quantitative measurements and scrupulous mathematical analyses will lead to a profound understanding of how neurons acquire polarity.

As this review focuses on models of neuronal symmetry-breaking, we could not cite many important studies reporting the molecules involved in neuronal polarization. We thank Dr. Ian Smith for reviewing the manuscript.

REFERENCES

Andersen SS, Bi GQ. 2000. Axon formation: a molecular model for the generation of neuronal polarity. Bioessays 22:172-179.

Arimura N, Kaibuchi K. 2007. Neuronal polarity: from extracellular signals to intracellular mechanisms. Nat. Rev. Neurosci. 8:194-205.

Barnes AP, Polleux F. 2009. Establishment of Axon-Dendrite Polarity in Developing Neurons. Annu. Rev. Neurosci. 32:347-381.

Bradke F, Dotti CG. 2000. Differentiated neurons retain the capacity to generate axons from dendrites. Curr. Biol. 10:1467-1470.

Bradke F, Dotti CG. 2000. Establishment of neuronal polarity: lessons from cultured hippocampal neurons. Curr. Opin. Neurobiol. 10:574-581.

Conde C, Caceres A. 2009. Microtubule assembly, organization and dynamics in axons and dendrites. Nat. Rev. Neurosci. 10:319-332.

Craig AM, Banker G. 1994. Neuronal polarity. Annu. Rev. Neurosci. 17:267-310.

Dotti CG, Sullivan CA, Banker GA. 1988. The establishment of polarity by hippocampal neurons in culture. J. Neurosci. 8:1454-1468.

Fivaz M, Bandara S, Inoue T, Meyer T. 2008. Robust neuronal symmetry breaking by Ras-triggered local positive feedback. Curr. Biol. 18:44-50.

Goslin K, Banker G. 1989. Experimental observations on the development of polarity by hippocampal neurons in culture. J. Cell Biol. 108:1507-1516.

Hodgkin AL, Huxley AF. 1952. The dual effect of membrane potential on sodium conductance in the giant axon of Loligo. J. Physiol. 116:497-506.

Hodgkin AL, Huxley AF. 1952. A quantitative description of membrane current and its application to conduction and excitation in nerve. J. Physiol. 117:500-544.

Iglesias PA, Devreotes PN. 2008. Navigating through models of chemotaxis. Curr. Opin. Cell Biol. 20:35-40.

Inagaki N, Chihara K, Arimura N, Menager C, Kawano Y, Matsuo N, Nishimura T, Amano M, Kaibuchi K. 2001. CRMP-2 induces axons in cultured hippocampal neurons. Nat. Neurosci. 4:781-782.

Jacobson C, Schnapp B, Banker GA. 2006. A change in the selective translocation of the Kinesin-1 motor domain marks the initial specification of the axon. Neuron 49:797-804.

Jiang H, Guo W, Liang X, Rao Y. 2005. Both the establishment and the maintenance of neuronal polarity require active mechanisms: critical roles of GSK-3beta and its upstream regulators. Cell 120:123-135.

Kishi M, Pan YA, Crump JG, Sanes JR. 2005. Mammalian SAD kinases are required for

neuronal polarization. Science 307:929-932.

Kondo S. 2002. The reaction-diffusion system: a mechanism for autonomous pattern formation in the animal skin. Genes Cells 7:535-541.

Kunda P, Paglini G, Quiroga S, Kosik K, Caceres A. 2001. Evidence for the involvement of Tiam1 in axon formation. J. Neurosci. 21:2361-2372.

Lamoureux P, Ruthel G, Buxbaum RE, Heidemann SR. 2002. Mechanical tension can specify axonal fate in hippocampal neurons. J. Cell Biol. 159:499-508.

Lewis J. 2008. From signals to patterns: space, time, and mathematics in developmental biology. Science 322:399-403.

Lewis J, Ozbudak EM. 2007. Deciphering the somite segmentation clock: beyond mutants and morphants. Dev. Dyn. 236:1410-1415.

Meinhardt H. 2008. Hans Meinhardt. Curr. Biol. 18:R401-402.

Meinhardt H, Gierer A. 2000. Pattern formation by local self-activation and lateral inhibition. Bioessays 22:753-760.

Menager C, Arimura N, Fukata Y, Kaibuchi K. 2004. PIP3 is involved in neuronal polarization and axon formation. J. Neurochem. 89:109-118.

Mogilner A, Wollman R, Marshall WF. 2006. Quantitative modeling in cell biology: what is it good for? Dev. Cell 11:279-287.

Mori T, Wada T, Suzuki T, Kubota Y, Inagaki N. 2007. Singar1, a novel RUN domain-containing protein, suppresses formation of surplus axons for neuronal polarity. J. Biol. Chem. 282:19884-19893.

Nishimura T, Yamaguchi T, Kato K, Yoshizawa M, Nabeshima Y, Ohno S, Hoshino M, Kaibuchi K. 2005. PAR-6-PAR-3 mediates Cdc42-induced Rac activation through the Rac GEFs STEF/Tiam1. Nat. Cell Biol. 7:270-277.

Samuels DC, Hentschel HG, Fine A. 1996. The origin of neuronal polarization: a model of axon formation. Philos. Trans. R. Soc. London B Biol. Sci. 351:1147-1156.

Schwamborn JC, Puschel AW. 2004. The sequential activity of the GTPases Rap1B and Cdc42 determines neuronal polarity. Nat. Neurosci. 7:923-929.

Shelly M, Lim BK, Cancedda L, Heilshorn SC, Gao H, Poo MM. 2010. Local and long-range reciprocal regulation of cAMP and cGMP in axon/dendrite formation. Science 327:547-552.

Shi SH, Jan LY, Jan YN. 2003. Hippocampal neuronal polarity specified by spatially localized mPar3/mPar6 and PI 3-kinase activity. Cell 112:63-75.

Shimada T, Toriyama M, Uemura K, Kamiguchi H, Sugiura T, Watanabe N, Inagaki N. 2008. Shootin1 interacts with actin retrograde flow and L1-CAM to promote axon outgrowth. J. Cell Biol. 181:817-829.

Sohrmann M, Peter M. 2003. Polarizing without a c(l)ue. Trends Cell Biol. 13:526-533.

Symons MH, Mitchison TJ. 1991. Control of actin polymerization in live and permeabilized fibroblasts. J. Cell Biol. 114:503-513.

Tahirovic S, Bradke F. 2009. Neuronal polarity. Cold Spring Harb. Perspect. Biol. 1:a001644.

Toriyama M, Sakumura Y, Shimada T, Ishii S, Inagaki N. 2010. A diffusion-based neurite length sensing mechanism involved in neuronal symmetry-breaking. Mol. Syst. Biol. 6:394.

Toriyama M, Shimada T, Kim KB, Mitsuba M, Nomura E, Katsuta K, Sakumura Y, Roepstorff P, Inagaki N. 2006. Shootin1: A protein involved in the organization of an asymmetric signal for neuronal polarization. J. Cell Biol. 175:147-157.

Wedlich-Soldner R, Li R. 2003. Spontaneous cell polarization: undermining determinism. Nat. Cell Biol. 5:267-270.

Weiner OD, Neilsen PO, Prestwich GD, Kirschner MW, Cantley LC, Bourne HR. 2002. A PtdInsP(3)- and Rho GTPase-mediated positive feedback loop regulates neutrophil polarity. Nat. Cell Biol. 4:509-513.

Yam PT, Wilson CA, Ji L, Hebert B, Barnhart EL, Dye NA, Wiseman PW, Danuser G, Theriot JA. 2007. Actin-myosin network reorganization breaks symmetry at the cell rear to spontaneously initiate polarized cell motility. J. Cell. Biol. 178:1207-1221.

Yoshimura T, Kawano Y, Arimura N, Kawabata S, Kikuchi A, Kaibuchi K. 2005. GSK-3beta regulates phosphorylation of CRMP-2 and neuronal polarity. Cell 120:137-149.

Zigmond SH, Levitsky HI, Kreel BJ. 1981. Cell polarity: an examination of its behavioral expression and its consequences for polymorphonuclear leukocyte chemotaxis. J. Cell Biol. 89:585-592.

FIGURE LEGENDS

Figure 1 Quantitative modeling of action potential. Hodgkin and Huxley quantified the dynamics of potassium conductance (A) and sodium conductance (B), and fitted them to mathematical models. When they then integrated both models (A and B) to compute action potential, the data obtained from the integrated model and experiment showed good agreement (C). Modified from Hodgkin and Huxley (1952b).

Figure 2 Two models for neuronal symmetry-breaking. (A) "One-takes-all" model. Each neurite competes for a limited amount of a molecule that induces neurite outgrowth. One of the neurites eventually wins in this competition (circular and thick arrows), leading to the depletion of the inducer in the cell body and the other neurites (thin arrows). (B) "Activator-inhibitor" model. An activator of neurite outgrowth becomes continuously activated within one neurite by a positive feedback loop (circular arrow), and this in turn generates an inhibitory signal for neurite outgrowth that propagates globally to the other neurites (white arrows).

Figure 3 Enhanced transport-based "One-takes-all" models. (A) Model of Samuels et al. A "determinant chemical" necessary for neurite outgrowth is transported from the cell body to the neurite tips (black arrows). The neurite outgrowth velocity (white arrows) positively correlates with the rate of the anterograde transport (dashed arrow). The anterograde transport constitutes a positive feedback loop with neurite outgrowth that amplifies the accumulation of the "determinant chemical" at the neurite tips. (B) Model of Fivaz et al. There is a positive feedback interaction between HRas and PI3K in neurite tips (circular arrows). The positive feedback between HRas and PI3K

enhances the anterograde transport of HRas (dashed arrow). As HRas activity induces neurite outgrowth, the enhancement of HRas transport and HRas-induced neurite outgrowth constitute an additional positive feedback loop for competitive accumulation of HRas.

Figure 4 Diffusion-based "one-takes-all" model. (A) A model for neurite length-dependent diffusion of shootin1 along the neurite shaft. C and C_0 represent shootin1 concentration in the growth cone and cell body, respectively. As molecules diffuse in proportion to the steepness of the concentration gradient (trapezoids), the diffusion rate is assumed to be proportional to C - C_0 and inversely proportional to the neurite length. (B) A model for diffusion-based neurite length-dependent shootin1 accumulation in growth cones. (C) Positive feedback interaction between length-dependent shootin1 accumulation and shootin1-induced neurite outgrowth. Modified from Toriyama et al. (2010).

Figure 5 Quantitative modeling of neurite length-dependent shootin1 accumulation. Intra-neuritic anterograde transport (A) and retrograde diffusion (B) of shootin1 were quantified, and fitted to mathematical models. The data in (A) show the timings of shootin1 arrival at growth cones and the relative amount of shootin1 observed in individual bolus arrivals. The data in (B) show the time course of shootin1 depletion in a growth cone by retrograde diffusion. (C) Shootin1 accumulation in growth cones, calculated by integrating the models in (A) and (B) (blue circles), was neurite length-dependent and showed good agreement with the experimental data (red circles). The data show the relationship between neurite length and shootin1 accumulation in

growth cones. Data of black spots with bars are means ± S.E. Modified from Toriyama et al. (2010).

Figure 6 Quantitative modeling of shootin1-induced neuronal symmetry-breaking. Shootin1 up-regulation (A) and shootin1-induced neurite outgrowth (B) were quantified, and fitted to mathematical models. These models were integrated with the model of neurite length-dependent shootin1 accumulation (C) in a model neuron where C and L represent shootin1 concentration in growth cone and neurite length, respectively (D). The combined model neuron spontaneously broke symmetry, in good agreement with the experimental data (E). Modified from Toriyama et al. (2010).

Inagaki Figure 1

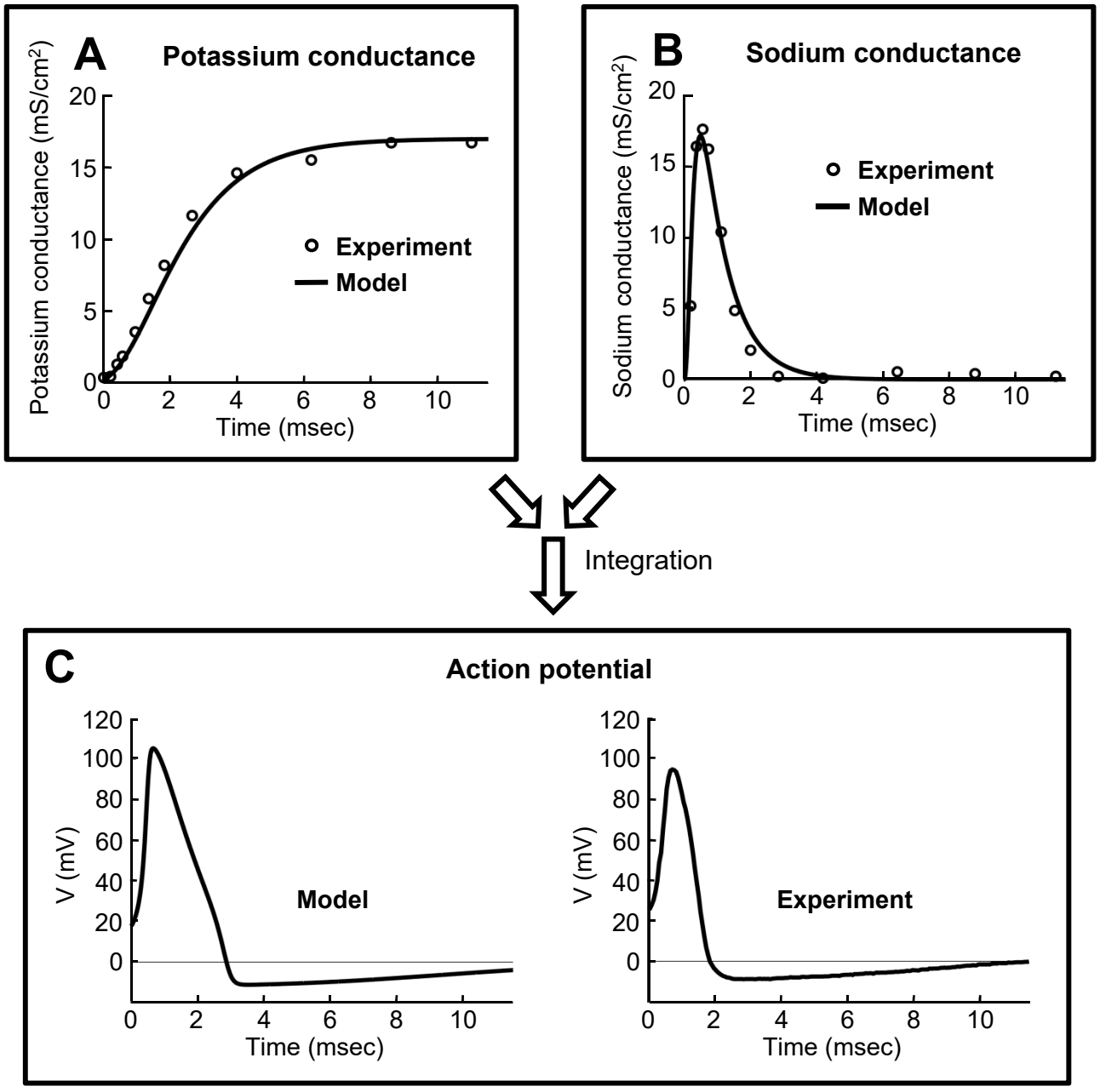

Inagaki Figure 2

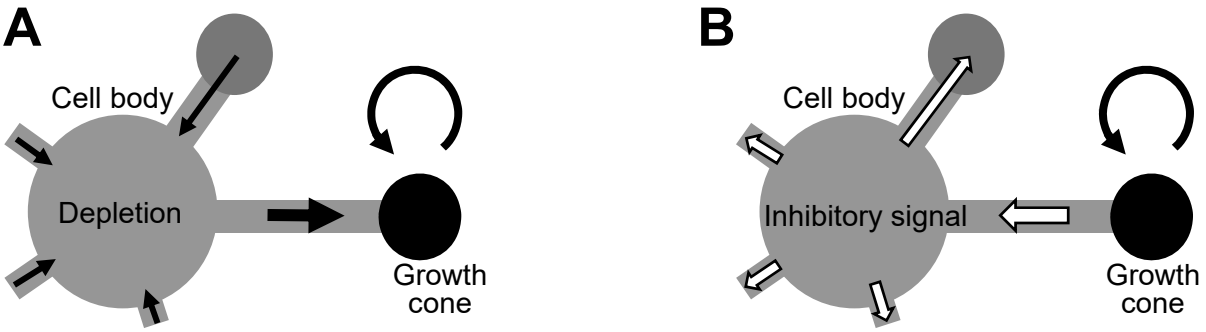

One-takes-all model

Activator-inhibitor model

Inagaki Figure 3

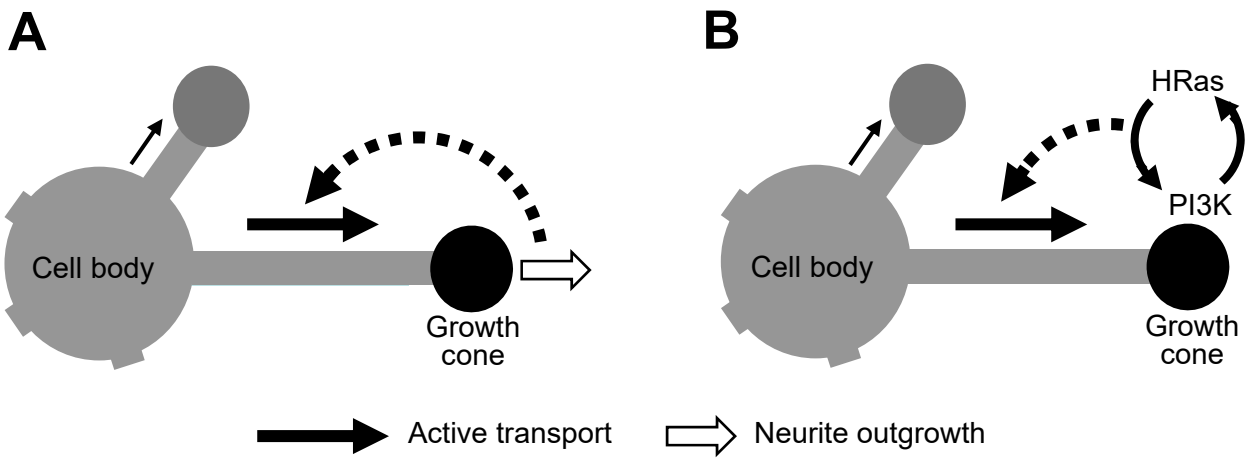

Inagaki Figure 4

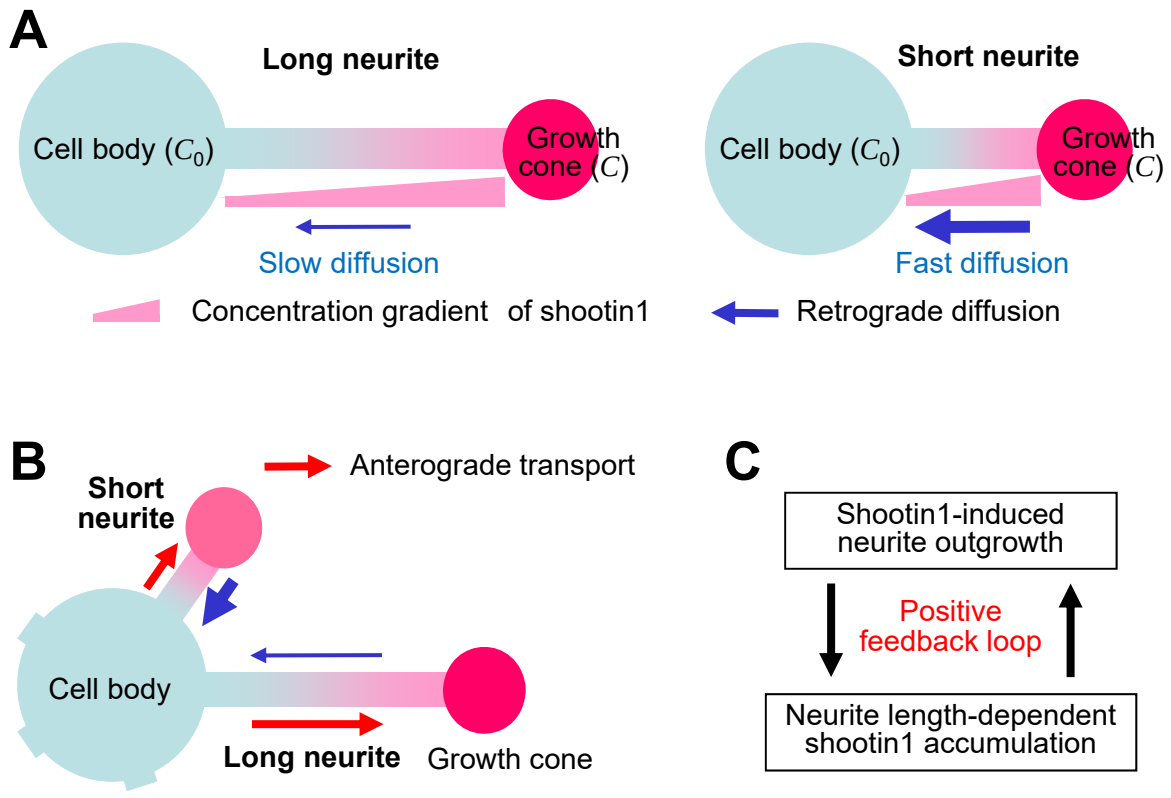

Inagaki Figure 5

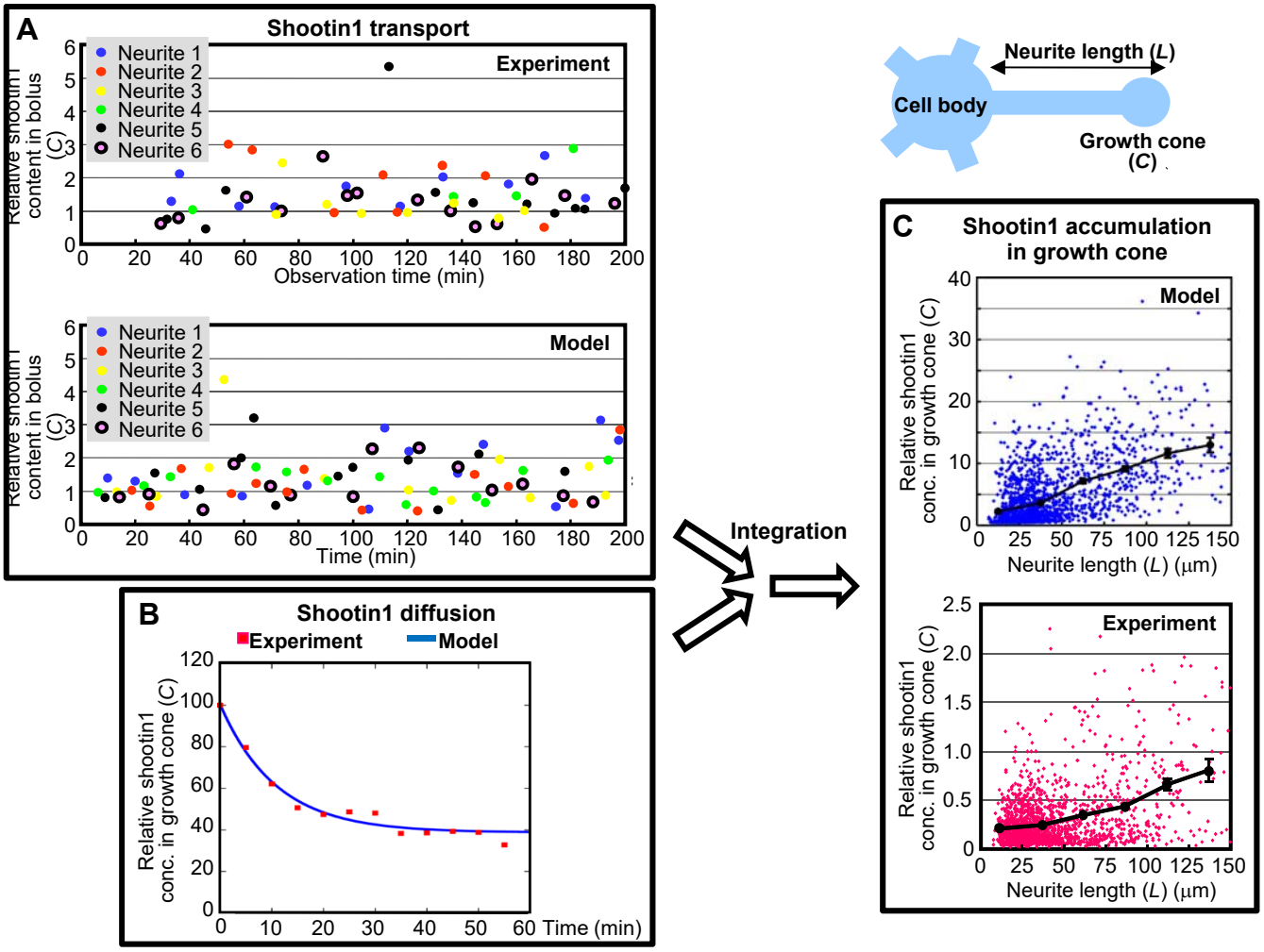

Inagaki Figure 6